

## The Hanle Effect as a Magnetic Diagnostic

Richard Ignace

*University of Wisconsin, Department of Astronomy, 5534 Sterling Hall,  
Madison, WI 53706, USA*

**Abstract.** The physics of the Hanle effect is briefly reviewed, and its application as a diagnostic of hot star magnetic fields is described. Emphasis is given to the practicalities of using spectropolarimetry of resolved wind emission lines to infer information about the circumstellar magnetic field strength and its geometry. A model for a weakly magnetized wind from “WCFields” theory is used as the backdrop for investigating polarized line profile effects for P Cygni resonance lines using a kind of “last scattering approximation”. Model results are presented for a typical P Cygni line that forms in a spherical wind. Significant line polarizations of a few tenths of a percent can result for circumstellar fields of order 100 G. Information about the field topology and surface field strength is gleaned from the Stokes- $Q$  and  $U$ -profiles. Simplistically, the  $Q$ -profile polarization is governed by the field strength, and the  $U$ -profile symmetry (whether symmetric or anti-symmetric or even zero) is governed by the field geometry.

### 1. Introduction

The Hanle effect is a magnetic field diagnostic that is still relatively unknown among stellar astronomers. The Effect refers to the modification (either an increase or decrease, as well as a change in position angle) of resonance line scattering polarization in the presence of a magnetic field, which begins to have an influence at fairly modest (even small) field strengths of just a few Gauss up to around 300 Gauss. Experiments to describe the polarization from resonance line scattering date back primarily to the early 1900’s (e.g., see Mitchell & Zemansky 1934). The influence of a magnetic field on the line polarization was explained first by a young physicist named Hanle for his dissertation (Hanle 1924). He described the effect of the magnetic field in semi-classical terms as arising from the precession of an atomic damped harmonic oscillator. Quantum mechanically, the Effect is understood in terms of an interference effect that occurs when the degeneracy of the magnetic sublevels in the excited level is partially lifted, and has applications to many topics in atomic physics (e.g., see the review by Moruzzi & Strumia 1991).

Astrophysically, the Hanle effect has been applied almost exclusively in the solar context, especially to measuring magnetic fields in the solar chromosphere and corona, and particularly in prominences and filaments (e.g., Lin, Penn, & Kuhn 1998). A detailed description of the physics of the Hanle effect and po-

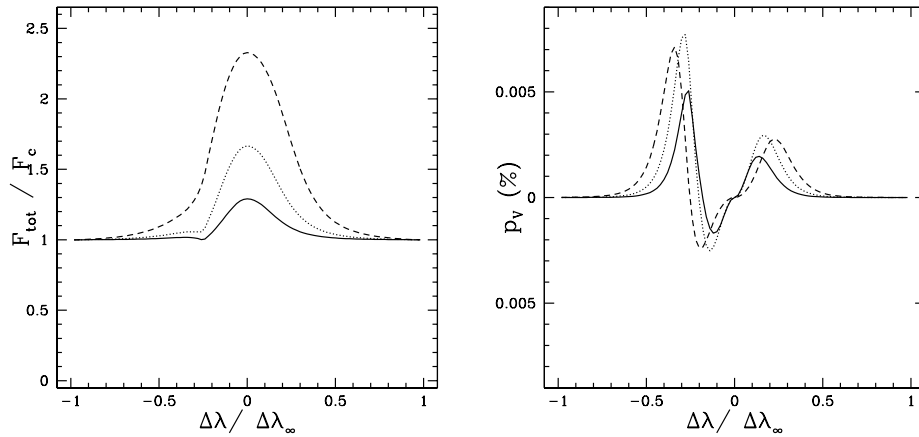


Figure 1. At left are continuum normalized recombination lines, each with a different line optical depth parameter, ranging from moderately thin to fairly thick. The magnetic field is assumed to be a split monopole threading a spherical wind in linear expansion ( $v(r) \propto r$ ). At right is the resulting Stokes- $V$  profile shown in percent polarization.

larized radiation transport with application to solar studies appears in Stenflo (1994). I began investigating the Hanle effect as a means for measuring circumstellar magnetic fields, especially in hot stars, as part of my graduate thesis (1996). This early work appears in Ignace, Nordsieck, & Cassinelli (1997), Ignace, Cassinelli, & Nordsieck (1999), and Ignace (2001). Development of the Hanle diagnostic continues, and here I wish to summarize its status, as well as observational prospects. First, I want to begin with a consideration of the more familiar Zeeman effect to use as a springboard for discussing the Hanle effect.

## 2. The Zeeman Effect for Detecting Circumstellar Magnetic Fields

The strength of the Zeeman effect and associated circularly polarized emission depends on the Zeeman splitting  $\Delta\lambda_B$ , as given by

$$\Delta\lambda_B = 4.67 \times 10^{-9} \mu\text{m} \cdot g_L \lambda^2 B, \quad (1)$$

with  $\lambda$  in microns,  $B$  in Gauss, and  $g_L$  the effective Lande factor to generalize the expression. A line in the visible band and a modest magnetic field of around 100 G yields a Zeeman splitting of a mere  $75 \text{ m s}^{-1}$ . This is considerably smaller than the thermal broadening typical of stellar envelopes, and much smaller than the velocity broadening in the winds, and this presents a serious difficulty: the circular polarizations of the two Zeeman split components are incoherent and oppositely signed, so that their broadening-induced overlap leads to severe polarimetric *cancellation*. What survives is a much weaker antisymmetric signal.

Following Stenflo (1994), and considering the fields to be “weak” (such that the Zeeman splitting is much less than the thermal broadening), the first order effect is the longitudinal Zeeman effect with Stokes  $V$  given by

$$V = -\Delta\lambda_B \cos\gamma \left( \frac{dI_0}{d\lambda} \right)_{\Delta\lambda} \quad (2)$$

where  $I_0$  is the intensity profile shape in the absence of a magnetic field and  $\cos\gamma = \hat{B} \cdot \hat{z}$ , for  $\hat{B}$  the magnetic field unit vector and  $\hat{z}$  a unit vector directed toward the observer. This expression indicates that the circular polarization will depend on the amount of the Zeeman shift, the orientation of the observer with respect to the vector magnetic field, and a gradient of the line profile function.

In the case of a stellar wind, standard expressions for Sobolev theory are adopted to describe the line profile formation (e.g., Mihalas 1978). An important concept in this theory is the “isovelocity zone”. All of the wind emission that appears at a given frequency in the line profile arises from a zone of fixed Doppler shift with respect to the observer. For example in a radially expanding wind, emission that appears at line center must arise from a surface coincident with the plane of the sky and passing through the center of the star, since the flow in that region has no velocity component along the line-of-sight.

The flux of circular polarization arising from the longitudinal Zeeman effect at a point in an isovelocity zone will depend on the line-of-sight gradient of the line source function and the line optical depth (see Ignace & Gayley 2003). The total polarized flux at a given line frequency then requires an integration over the entire isovelocity zone. Figure 1 shows an example for mildly thick recombination lines. The abscissa for each plot is the wavelength shift  $\Delta\lambda$  from line center as normalized by the maximum shift for the terminal speed flow  $\Delta\lambda_\infty = \lambda_0 v_\infty / c$ . At left is the continuum normalized flux, the three lines being for different optical depths. At right is the Stokes- $V$  polarization with  $p_V = F_V / F_{tot}$ . The percent polarizations are *extremely* small, at less than 0.01%! These low values result primarily from the fact that the gradient factor introduces a scaling that is inversely proportional to the line broadening, which in this case is  $\Delta\lambda_B / \Delta\lambda_\infty \ll 1$ . In contrast, the Hanle effect is a different method for measuring magnetic fields that is especially well-suited for the circumstellar case.

### 3. Physics of the Hanle Effect

It should be stressed again that the Hanle effect is a *modification* of the linear polarization that arises from resonance line scattering. Semi-classically, line scattering can be split into two parts: an isotropic scattering component and a dipole scattering component, like free electrons (e.g., Hamiton 1947; Chandrasekhar 1961). The fraction of the scattering that is dipole-like is referred to as the “polarizability”,  $E_1$ ; the isotropic scattering contribution is given fractionally as  $(1 - E_1)$ .

One can think of resonance scattering in terms of a damped harmonic oscillator. Suppose that a beam of polarized intensity (100%) impinges on a sample of scatterers. The oscillators are excited and oscillate parallel to the sense of the beam polarization, scattering light anisotropically (with peak intensity perpendicular to the direction of oscillation and zero intensity along that direction).

The introduction of a magnetic field induces a precession of the oscillators. There are two important points here. (a) The atomic oscillators no longer “bob” in a fixed direction. Instead, they begin to oscillate in directions perpendicular to

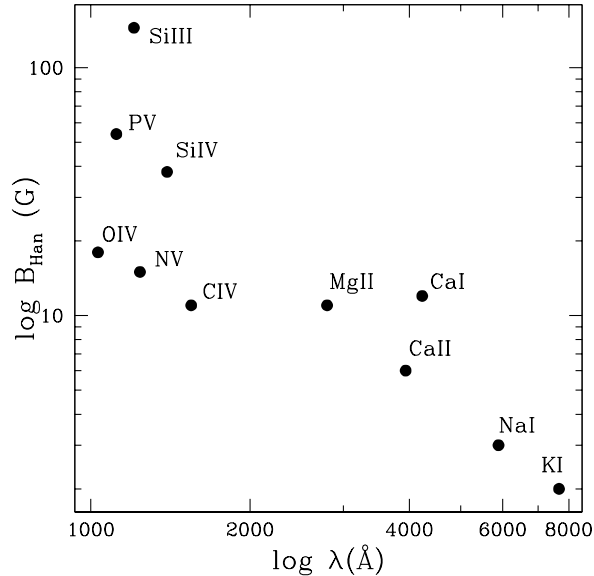


Figure 2. Plotted is the logarithm of the Hanle field sensitivity  $B_{Han}$  against line wavelength. The Hanle field is defined such that  $2g_L\omega_L/A = B/B_{Han} = 1$ . The ion yielding each resonance line is indicated. The CaI and SiIII lines are singlets; the rest are Li-like doublets. Low ionization optical lines are sensitive to fields in the 1-10 G range, whereas high ionization UV lines are sensitive to stronger fields in the 10-100 G range.

the polarization of the incident light. Consequently, one can think of the Hanle effect as redistributing energy between orthogonal axes of atomic oscillation. (b) The oscillators are damped, emitting their absorbed radiation at a rate given by the Einstein  $A$ -value for the transition of interest. Magnetic precession occurs at a rate given by the Larmor frequency,  $\omega_L = eB/m_e c$ . Hence there will be a Hanle effect only if these two rates are similar. I define the ‘‘Hanle ratio’’ as

$$\frac{g_L\omega_L}{A} = g_L \frac{(B/10 \text{ G})}{(A/10^8 \text{ s}^{-1})}. \quad (3)$$

Typical strong lines are sensitive to the Hanle effect for field strengths in the 1-300 G range (see Fig. 2). Note also that different lines will have different Hanle sensitivities. Finally, if the Hanle ratio is small, the scattering is essentially non-magnetic (i.e., little precession occurs over the lifetime of the level), but if the ratio is large, the Hanle effect is said to be ‘‘saturated’’. Saturated means that the precession is so rapid that little damping of the oscillators occurs after one full rotation, so that to increase the field will not alter the Hanle effect. Diagnostically, one loses sensitivity to the field strength, but the scattering polarization still depends on the vector orientation of the magnetic field. Of

course, if the field becomes very large indeed, the scattering physics shifts from the Hanle effect to the Zeeman effect.

#### 4. Application of the Hanle Effect to P Cygni Lines

There are two main differences that distinguish the use of the Hanle effect in studies of the Sun versus hot stars. The first is the fact that the Sun is a resolved source, and stars are not. Cassinelli, Nordsieck, & Ignace (2001) have also pointed out that in the hot star wind case, the lines are strongly NLTE and relatively simple to treat, and the scattering is of a “flat” stellar continuum, whereas neither of these is the case for most applications of the Hanle effect in the Sun. So to compute polarized profiles of *wind emission lines*, standard Sobolev theory is once again adopted. For resonance scattering lines, Sobolev theory yields P Cygni line profiles that are commonly observed from stellar winds (see Lamers & Cassinelli 1999).

##### 4.1. The Single Scattering Approximation

The single scattering approximation is simply a physically motivated convenience whereby the line emission from optically thick portions of the wind is assumed to be completely unpolarized, and the emission from optically thin portions is assumed to be described by the source functions given in Ignace (2001). The multiple scattering in thick regions is expected to be depolarized, whereas multiple scattering does not occur in thin regions. This approach is closely related to the “last scattering approximation” that is sometimes employed for static media.

##### 4.2. WCFields Primer

A realistic model for a magnetized wind is required to produce synthetic polarized line profiles. WCFields is an axisymmetric semi-analytic model for just such a wind that is based on “wind compression” (WC) theory. In WC theory (Bjorkman & Cassinelli 1993; Ignace, Cassinelli, & Bjorkman 1996), the wind flow from a rotating star is described kinematically. Ignoring pressure gradient terms, and assuming radial wind-driving forces, one can derive an expression for the streamline flow. The general properties of WC theory have been confirmed with hydrodynamic simulations by Owocki, Cranmer, & Blondin (1994), although the effects appear to be inhibited when non-radial accelerations that arise in the line-driving of hot star winds are included (Owocki, Cranmer, & Gayley 1996).

However, retaining the basic elements of WC theory, Ignace, Cassinelli, & Bjorkman (1998) extended the method to allow for “weak” magnetic fields. The key assumptions are that the magnetic field is frozen-in and dominated by the hydrodynamic flow. Consequently, the known flow geometry determines the magnetic field topology. Referring to Ignace et al. (1998) for the derivation, the expression that determines the vector magnetic field throughout the flow is

$$\mathbf{B} = B_* \left( \frac{R_*^2}{r^2} \right) \left( \frac{d\mu}{d\mu_0} \right)^{-1} \frac{\mathbf{V}}{v_r}, \quad (4)$$

where  $B_*$  is the surface field strength,  $d\mu/d\mu_0$  is the “compression factor” that describes how neighboring streamlines evolve throughout the wind flow,  $\mathbf{V}$  is the vector velocity in the co-rotating frame, and  $v_r$  is the radial velocity. All of the velocity components and the compression factor are knowns. The scalar strength of the field is given by

$$B = B_* \left( \frac{R_*^2}{r^2} \right) \left( \frac{d\mu}{d\mu_0} \right)^{-1} \sqrt{1 + \frac{v_{\text{rot}}^2}{v_r^2} \left( \frac{R_*}{r} \sin \vartheta_0 - \frac{r}{R_*} \sin \vartheta \right)^2}, \quad (5)$$

where  $v_{\text{rot}}$  is the equatorial rotation speed of the star. The zero subscript indicates a value at the base of the wind. The latitude of a streamline varies with radius as flow migrates toward the equator from both the upper and lower hemispheres. The field is taken to be radial at the wind base, but obtains a toroidal configuration at large radius, with  $B \propto r^{-1} \sin \vartheta$ , like the magnetic field that is dragged out in the solar wind. For the slow rotations that will be considered here, the factor  $d\mu/d\mu_0$  varies little from pole to equator and so is ignored. Additionally,  $B_\vartheta$  is generally smaller than either  $B_r$  or  $B_\varphi$ , and is also ignored. The resulting model is a spherically symmetric wind with a complex radial and toroidal magnetic field morphology.

### 4.3. Model Line Profile Results

Using WCFields theory for slowly rotating stars, polarized emission profiles from P Cygni lines have been computed and are shown in Figure 3. The rotation was chosen to be 8% of the terminal speed. Since most O star winds have terminal speeds of around  $2000 \text{ km s}^{-1}$ , the equatorial rotation speed would be around  $150 \text{ km s}^{-1}$ , which is not atypical of observed  $v \sin i$  values (Penny 1996). Especially important is the fact that the wind is assumed to be spherically symmetric. In WCFields theory, this model would have a mild equator-to-pole density contrast of 1.25 asymptotically. The wind is taken to be explicitly spherical to isolate the influence of the Hanle effect, since an unresolved spherically symmetric distribution of scatterers would otherwise yield no net polarization. The different profiles are for different surface field strengths as indicated. The upper frames are for the Stokes  $Q$  profile, and the lower for Stokes  $U$ .

The left panels are for the wrong field topology and the right is for the correct one. The wrong case assumes a surface magnetic field that is initially outward radial – a monopole, which violates the condition  $\nabla \cdot \mathbf{B} = 0$  over a closed surface. The panels at right are for a surface field that is initially a split monopole, with field lines outward radial in the upper hemisphere and inward radial in the lower hemisphere. In every case the star is viewed as edge-on.

The two cases are shown to illustrate how the Hanle effect can be used to glean information about the magnetic field. What is immediately striking is that the surface monopole case yields a net  $U$ -profile, whereas the surface split monopole case does not. So the  $U$ -profile is a sensitive probe of the field symmetry (such as top-bottom and left-right).

The  $Q$ -profile also depends on the field symmetry, but simplistically, the  $Q$ -profile shows stronger polarizations for larger surface fields, and can thus be considered a gauge of the surface field strength. Note that the surface fields rise

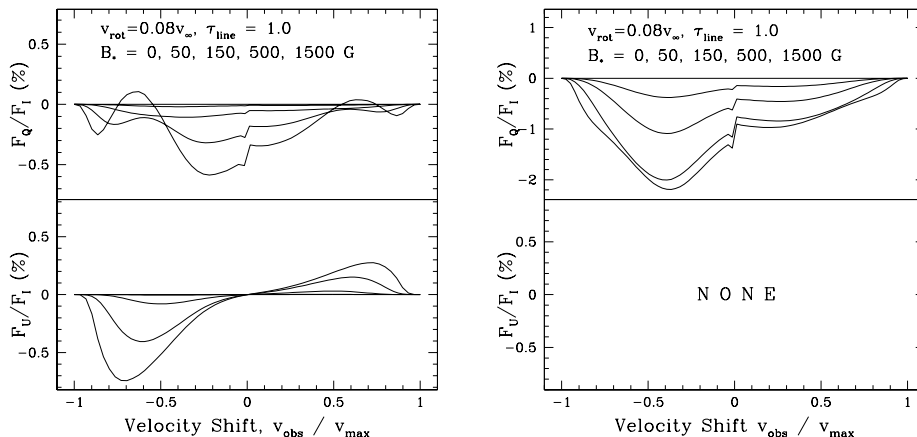


Figure 3. Shown are Stokes  $Q$  and  $U$  polarized line profiles for *spherical* winds and WCFields magnetic geometries. The stellar rotation, which determines the field topology, is fixed at 8% of the terminal speed, and the star is viewed from an equator-on perspective. Each line is for a different surface field strength as indicated, with higher fields producing stronger line polarizations. The only difference between the left and right is that in former, the surface field is initially a monopole, and in the latter it is a split monopole. Consequently, the  $U$ -profile is quite sensitive to the symmetry of the field topology, whereas the  $Q$ -polarization generally grows with surface field strength.

up to 1500 G in these examples. Such large values are beyond the Hanle effect and firmly in the Zeeman regime (Stenflo 1998). However, in these models, the inner wind is quite optically thick in the line opacity, and only the outer wind is thin (e.g., some portions of the wind start to become thin around  $2R_*$ ). It is only these thin portions that contribute to the Hanle effect in the single scattering approximation, and at these radii the field is considerably reduced relative to the surface value.

In summary, significant linear polarizations in the line of a few tenths of a percent can result from the Hanle effect, and the influence of the line optical depth is to ensure that for typical P Cygni lines, the Hanle effect will probe circumstellar magnetic fields at intermediate radii of a few  $R_*$  in the wind, even if the wind is spherical. For cases when the wind is distorted from spherical, as one would expect from a magnetized flow, polarizations from more than one line, each having a different Hanle sensitivity, will generally be needed to disentangle the effects of the magnetic field from that of the non-spherical geometry.

### 5. Observational Prospects

The Far Ultraviolet SpectroPolarimeter (FUSP) is a sounding rocket payload that is expected to launch in autumn 2003. The goal of the mission will be to make spectropolarimetric measurements in the wavelength range of 1050–1500 Å for several different targets (see Tab. 1). With a 50 cm primary, the instrument

Table 1. Some FUSP Targets

Star	V	$m_{133}^a$	Comment
$\zeta$ Ori	2.1	-2.5	<b>Target for Hanle effect</b>
$\gamma$ Cas	2.5	-1.6	Be star
$\zeta$ Tau	3.0	-0.3	Be star
$\xi$ Per	4.0	1.0	O7e rapid rotator
HD 93521	7.1	2.8	O9e rapid rotator
EZ CMa	6.9	2.5	Wolf-Rayet star
$\beta$ Ori	0.1	-0.8	Supergiant star
$\beta$ Lyr	3.5	2.0	Binary system

<sup>a</sup> Apparent magnitude at 133 nm

will have a spectral resolution of  $0.65 \text{ \AA}$ , corresponding to  $\lambda/\Delta\lambda = 1800$  at a wavelength of  $1170 \text{ \AA}$ . This in turn corresponds to a velocity resolution of about  $170 \text{ km s}^{-1}$ , which is sufficient to resolve wind-broadened lines with typical full widths of a few thousand  $\text{km s}^{-1}$ . Targeting the star  $\zeta$  Ori, which was observed in the FUV with Copernicus, it is anticipated that FUSP will produce the first detection of the Hanle effect in a star other than the Sun.

## 6. Concluding Remarks

This contribution has focussed on the Hanle effect in resonance scattering lines common to hot star winds. The study of the Effect and the development of radiative transport techniques is ongoing, especially in terms of relaxing the single scattering approximation for the line polarization. The description presented here ignores the influence of nuclear spin for the polarizability  $E_1$  of a particular transition, but nuclear spin can have a significant effect on its value (e.g., Nordsieck 2001). We have also ignored the influence of fluorescent alignment, which affects the populations of the magnetic sublevels. Fluorescent alignment is also subject to magnetic “re-alignment” effects, which are related to the Hanle effect and operate at much weaker field strengths (see Nordsieck 2001). We are investigating the regime in which the Hanle effect and the magnetic re-alignment physics both apply.

**Acknowledgments.** I want to thank Joe Cassinelli and Ken Nordsieck for helpful suggestions in preparing this presentation. Support for this research comes from a grant from the National Science Foundation (AST-0098597).

## References

- Bjorkman, J. E., & Cassinelli, J. P. 1993, ApJ, 409, 429  
 Cassinelli, J. P., Nordsieck, K. H., & Ignace, R. 2001, in Magnetic Fields Across the Hertzsprung-Russell Diagram, ASP Conf. 248, ed. G. Mathys, S. Solanki, & D. Wickramasinghe (San Francisco: ASP), 409  
 Chandrasekhar, S. 1960, Radiative Transfer (New York: Dover)  
 Hamilton, D. R. 1947, ApJ, 106, 457



- Hanle, W. 1924, *Z. Phys.*, 30, 93
- Ignace, R. 1996, Ph.D. Thesis, Univ. Wisconsin
- Ignace, R., Cassinelli, J. P., & Bjorkman, J. E. 1996, *ApJ*, 459, 671
- Ignace, R., Nordsieck, K. H., & Cassinelli, J. P. 1997, *ApJ*, 486, 550
- Ignace, R., Cassinelli, J. P., & Bjorkman, J. E. 1998, *ApJ*, 505, 910
- Ignace, R., Cassinelli, J. P., & Nordsieck, K. H. 1999, *ApJ*, 520, 335
- Ignace, R. 2001, *ApJ*, 547, 393
- Ignace, R., & Gayley, K. G. 2003, *MNRAS*, in press
- Lamers, H. J. G. L. M., & Cassinelli, J. P. 1999, *Introduction to Stellar Winds* (Cambridge: University Press)
- Lin, H., Penn, M. J., & Kuhn, J. R. 1998, *ApJm*, 493, 978
- Mihalas, D. 1978, *Stellar Atmospheres* (San Francisco: Freeman)
- Mitchell, A. C. G., & Zemansky, M. W. 1934, *Resonance Radiation and Excited Atoms* (Cambridge: University Press)
- Moruzzi, G., & Strumia, F., eds. 1991, *The Hanle Effect and Level-Crossing Spectroscopy* (New York: Plenum Press)
- Nordsieck, K. H. 2001, in *Magnetic Fields Across the Hertzsprung-Russell Diagram*, ASP Conf. 248, ed. G. Mathys, S. Solanki, & D. Wickramasinghe (San Francisco: ASP), 607
- Owocki, S. P., Cranmer, S. R., & Blondin, J. M. 1994, *ApJ*, 424, 887
- Owocki, S. P., Cranmer, S. R., & Gayley, K. G. 1996, *ApJ*, 472, L115
- Penny, L. R. 1996, *ApJ*, 463, 737
- Stenflo, J. O. 1994, *Solar Magnetic Fields* (Dordrecht: Kluwer)
- Stenflo, J. O. 1998, *A&A*, 338, 301

## Discussion

*Wade:* The Hanle effect is certainly observed in optical lines in the solar spectrum. Why do you need to go to the FUV for hot stars?

*Ignace:* The answer comes down to suitable lines for suitable stars. For hot stars, most of the flux is in the UV, and spectropolarimetry requires lots of photons. Moreover, the Einstein  $A$ -values that set the scale for the magnetic field sensitivity are greater for shorter wavelength lines, so that UV lines are sensitive to  $\sim 10-300$  G fields, but optical lines to  $\sim 1-10$  G. Finally, strong resonance scattering lines are found only in the UV for hot stars (e.g., NV, CIV, etc), whereas the optical spectrum will have photospheric absorption or recombination emission lines. Optical lines like NaI and CaII can show a Hanle effect, but these low ions do not exist in hot stars.